Contents lists available at ScienceDirect

Clinica Chimica Acta

journal homepage: www.elsevier.com/locate/cca

Salivary proteomic analysis in asymptomatic and symptomatic SARS-CoV-2 infection: Innate immunity, taste perception and FABP5 proteins make the difference

Ada Aita [a,1], Ilaria Battisti [b,c,1], Nicole Contran [a,1], Serena Furlan [c], Andrea Padoan [a], Cinzia Franchin [b,c], Francesco Barbaro [d], Anna Maria Cattelan [d], Carlo-Federico Zambon [a], Mario Plebani [a], Daniela Basso [a,*], Giorgio Arrigoni [c,e]

[a] Department of Medicine, University of Padova, Padova, Italy
[b] Department of Agronomy, Food, Natural Resources, Animals and Environment, University of Padova, Padova, Italy
[c] Proteomic Center of Padova University and Azienda Ospedaliera di Padova, Padova, Italy
[d] Tropical and Infectious Diseases Unit, University Hospital of Padova, Padova, Italy
[e] Department of Biomedical Sciences, University of Padova, Padova, Italy

ABSTRACT

Background and aim: SARS-CoV-2 infection spawns from an asymptomatic condition to a fatal disease. Age, comorbidities, and several blood biomarkers are associated with infection outcome. We searched for biomarkers by untargeted and targeted proteomic analysis of saliva, a source of viral particles and host proteins.
Methods: Saliva samples from 19 asymptomatic and 16 symptomatic SARS-CoV-2 infected subjects, and 20 controls were analyzed by LC-MS/MS for untargeted peptidomic (flow through of 10 kDa filter) and proteomic (trypsin digestion of filter retained proteins) profiling.
Results: Peptides from 53 salivary proteins were identified. ADF was detected only in controls, while IL1RA only in infected subjects. PRPs, DSC2, FABP5, his-1, IL1RA, PRH1, STATH, SMR3B, ANXA1, MUC7, ACTN4, IGKV1-33 and TGM3 were significantly different between asymptomatic and symptomatic subjects. Retained proteins were 117, being 11 highly different between asymptomatic and symptomatic (fold change ≥2 or ≤−2). After validation by LC-MS/MS-SRM (selected reaction monitoring analysis), the most significant discriminant proteins at PCA were IL1RA, CYSTB, S100A8, S100A9, CA6, and FABP5.
Conclusions: The differentially abundant proteins involved in innate immunity (S100 proteins), taste (CA6 and cystatins), and viral binding to the host (FABP5), appear to be of interest for use as potential biomarkers and drugs targets.

1. Introduction

Within a few months of its inception, the novel coronavirus Severe Acute Respiratory Syndrome Coronavirus-2 (SARS-CoV-2) causing serious coronavirus disease 2019 (COVID-19) became a health emergency worldwide [1,2]. The clinical presentation of SARS-CoV-2 infection ranges from asymptomatic or pauci-symptomatic infection (50–75 % of subjects) with mild, transitory symptoms to severe disease (25–50 %). The mortality rate in patients with severe disease is in the region of 25 %, and in patients on mechanical ventilation in intensive

care, the overall case-fatality rate ranges from 3 to 15 % depending upon the age of the patient and the presence of co-morbidity (e.g. diabetes, cardiovascular diseases, hypertension and cancer) [3–7]. The mass vaccination program together with the emergence of SARS-CoV-2 variants have modified the clinical pattern, asymptomatic or pauci-symptomatic infection occurring in the vast majority of cases. However even actually in the course of the fifth wave, severe diseases and mortality continues to occur [8]. Although considerable progress has been made detecting of SARS-CoV-2 infection and understanding its pathogenesis and host response, and despite currently available routine laboratory tests which make an important contribution to its diagnosis, it remains difficult to predict the host response to infection and to establish the disease prognosis. Proteomics appears a promising tool for screening markers of disease occurrence and progression through the differential expression of proteins.

Proteomic profiling has been used to differentiate COVID-19 patients from healthy subjects and/or to understand the host response to SARS-CoV-2 infection in urine samples [9] and naso-pharyngeal swabs (NPS) [10]. Furthermore, a mass spectrometry-based approach has been employed to predict the severity of COVID-19 in peripheral blood plasma [11]. Blood and urine samples are frequently used to search for new biomarkers since they are non-invasive and easy to collect. Studies using NPS, the standard sampling method for diagnosing COVID-19, should be considered since they might evidence first line defense against pathogens.

Recently we and others proposed saliva, considered the main vehicle of viral spread, as a valid and attractive alternative to NPS in SARS-CoV-2 detection, since it is self-collected at home with an easy and standardized procedure that provides a pure sample, which is easy to handle in the laboratory [12–15]. Furthermore, as it is a plasma ultrafiltrate, saliva can be considered a viable alternative to blood for the measurement of protein markers. As yet, however, no systematic investigation has been undertaken into salivary proteomic alterations due to SARS-CoV-2 infection. The resident microbiome and proteases might affect saliva sample stability causing protein degradation during collection and within few hours after sample collection [16]. An integrated approach aiming to evaluate both peptides and proteins in saliva might therefore be conducive to discovering new potential biomarkers, and new molecular pathways involved in disease pathogenesis and outcome [16].

The aim of the present study was to analyse the saliva peptidome and proteome in asymptomatic and symptomatic COVID-19 patients using high throughput proteomics techniques, MS profiling, untargeted and targeted LC-MS/MS approaches in order to identify putative biomarkers implicated in different host responses to the virus.

2. Study population

This retrospective study was conducted on a total of 55 saliva samples collected from August to November 2020. Twenty samples were from outpatients screened for suspected SARS-CoV-2 (i.e. contact with a SARS-CoV-2 positive subject or with typical symptoms) and resulted negative at molecular testing (controls group: C), while 35 were from SARS-CoV-2 positive subjects. Infected subjects were subdivided in two groups: A) asymptomatic group including 19 (7F, 12M; age range, 25–62 years) University employees participating in an active surveillance program based on saliva molecular testing with a RT-PCR positive result on saliva, confirmed on NPS molecular testing the subsequent day. All of them were asymptomatic or pauci-symptomatic; S) symptomatic group including the remaining 16 subjects (5F, 11M; age range, 28–88 years) who were COVID-19 inpatients hospitalized in the Tropical and Infectious Disease Unit at the University-Hospital of Padova.

After giving their fully informed consent in writing (Local Ethic Committee Nr. 27444), each patient was asked to collect a morning saliva sample (Salivette device, SARSTEDT AG & Co, Nümbrecht, Germany) as previously detailed [12].

3. Sample collection and analysis

Saliva, collected after overnight fasting using a standardized procedure by a barcoded Salivette®, was centrifuged at 4000 g for 5 min.

3.1. Molecular testing

SARS-CoV-2 RNA was obtained from 200 μL of saliva by automated nucleic acid extraction, using the Roche MagNA Pure 96 Instrument with the MagNA Pure 96 DNA and Viral NA Small Volume Kit (pathogen universal 200 protocol). RNA was amplified by QuantStudio™ five Real-Time PCR Systems (Applied Biosystems, USA) using TaqPath COVID-19 CE-IVD RT-PCR kit (Life Technology, Applied Biosystems, USA) as described elsewhere [17]. The TaqPath COVID-19 RT-PCR kit has CE-IVD certification for the usage of salivary samples. All 35 saliva samples obtained from infected (asymptomatic and symptomatic) subjects were positive at rRT-PCR analysis for SARS-CoV-2.

3.2. Sample preparation, TMT-labelling and SCX

Salivary samples were stored at $-80\,^\circ$C within 24 h from collection. Protein quantification was performed using the Bradford method on all saliva samples and an average protein concentration of $\approx$1 μg/μL (Mean $\pm$ SE = 1.01 $\pm$ 0.05) was detected. To standardize the analysis, the same volume of each sample was used. We chose to use an isovolumetric approach rather than a method based on the same protein quantity because the variations in protein content were limited and a protein content approach might mask differences between subjects that could be of relevance in clinical translation, a setting where it would be much more convenient to prepare the samples by simply measuring a certain volume of saliva rather than measuring first the protein concentration and then, based on the results, the adequate sample volume for the analysis.

Briefly, 30 μL of each saliva sample were diluted in 200 μL with the washing buffer (WB, Urea 8 M, Tris-HCl 100 mM, pH 8.5) and loaded into a Vivacon 500 filter (Sartorius, Germany) with a molecular cut-off of 10 kDa to perform a FASP (Filter Aided Sample Preparation) protocol for protein digestion. Three washes with WB and subsequent centrifugation at 18,600×g were performed. The flow-through was collected to recover salivary endogenous peptides which were then desalted using C18 cartridges (Sep-Pak, Waters, USA), dried under vacuum and stored at $-20\,^\circ$C for further analysis. Proteins retained in the filter were reduced with 50 mM dithiothreitol (Fluka) in WB (incubation at 55 $^\circ$C for 30 min) and alkylated with 50 mM iodoacetamide (Sigma, Italy) in WB (incubation 20 min at room temperature and in the dark). Proteins were washed twice with WB, once with NH_4HCO_3 100 mM and once with NH_4HCO_3 50 mM, as previously described [18]. Protein digestion was performed overnight at 37 $^\circ$C adding 0.6 μg of sequencing grade modified trypsin (Promega, USA). Three extraction steps performed by washing with 50 mM NH_4HCO_3 and centrifuging at 18,600×g for 10 min, allowed to collect peptides that were finally acidified to pH 3 with formic acid, dried under vacuum and stored at $-20\,^\circ$C.

Untargeted peptidomic and proteomic studies described below were performed not on individual samples but using samples pools. Dried samples of endogenous peptides were suspended in 9 μL of 10 % acetonitrile (ACN)/0.1 % formic acid (FA) and then diluted with 0.1 % FA to a final volume of 36 μL. Four to five individual saliva samples from each study group (controls, asymptomatic and symptomatic) were randomly selected and mixed, creating four pools of 15 μL each (Table 1). Tryptic peptides were suspended in 30 μL of water, and mixed according to the scheme reported in Table 1 to create pools of 40 μL. These were then diluted with 0.1 % FA to a final volume of 1 mL, desalted with C18 cartridges (Sep-Pak, Waters) and dried under vacuum.

Pools of tryptic peptides were suspended in 50 μL of 100 mM triethyl ammonium bicarbonate (TEAB, Sigma) and labelled with Tandem Mass Tags (TMT, Thermo Fisher Scientific) following manufacturer's

Table 1
Pool preparation. The table describes how individual samples were mixed to prepare the different pools of saliva samples belonging to the three groups of control (pools C1–C4), asymptomatic (pools A1–A4) and symptomatic (pools S1–S4) subjects.

Pool C	Control Samples number	Pool A	Asymptomatic Samples number	Pool S	Symptomatic Samples number
Pool C1	114, 133, 155, 160, 163	Pool A1	2, 7, 10, 15, 17	Pool S1	34, 51, 92, 95
Pool C2	115, 136, 156, 61, 189	Pool A2	1, 3, 9, 18, 20	Pool S2	64, 99, 124, 211
Pool C3	116, 139, 157, 188, 190	Pool A3	4, 6, 11, 13, 19	Pool S3	60, 72, 195, 219
Pool C4	134, 137, 158, 159, 191	Pool A4	5, 12, 14, 16	Pool S4	67, 79, 145, 210

instructions. Briefly, 8 μL of each TMT label (0.8 mg in 40 μL of ACN) was added to each sample and the reaction was allowed to proceed at room temperature for 1 h and then quenched by the addition of 8 μL of 5 % (w/v) NH$_2$OH. To assess the completeness of the labeling, individual samples were analyzed by liquid chromatography-tandem mass spectrometry (LC-MS/MS) as detailed below. Data were searched with the Mascot search engine setting TMT labeling as variable modification: all identified peptides were correctly modified at the N-terminus and each lysine residue, thus confirming the efficiency of the labelling procedure. Labelled samples were mixed (C1, C4, A2, A3, S1, S3 for replicate 1 and C2, C3, A1, A4, S2, S4 for replicate 2) and the excess of tags was removed by strong cation exchange chromatography (SCX) using a single elution step with 350 mM KCl, as described elsewhere [18]. Samples were finally desalted (C18, Sep-Pak), dried under vacuum and stored at −20 °C until LC-MS analysis was performed.

3.3. Untargeted proteomic analysis

Untargeted peptidomic and proteomic analyses were performed by LC-MS/MS with an LTQ-Orbitrap XL mass spectrometer (Thermo Fisher Scientific, USA) coupled online with a nano-HPLC Ultimate 3000 (Dionex – Thermo Fisher Scientific, USA).

The analysis of endogenous peptides was carried out with a label-free approach. Peptides were separated in a 10 cm pico-frit column (75 μm I.D., New Objectives), packed in-house with C18 material (Aeris Peptide 3.6 μm XB-C18, Phenomenex) using a flow rate of 250 nL/min and a linear gradient of ACN from 3 % to 40 % in 40 min. A Top10 data dependent acquisition method was applied, consisting in a full MS scan in the range 300–1700 *m/z* in the Orbitrap (60,000 nominal resolution) followed by MS/MS scans in the linear trap (CID fragmentation) of the ten most intense ions. Two technical replicates were acquired for each sample with a randomized approach.

Raw files were analyzed with the MaxQuant – Andromeda search engine [19] against the Human section of Uniprot Database (version Sept2020) [20] to which protein sequences of SARS-CoV-2 were added. An unrestricted search was performed (no enzyme), setting as variable modification the oxidation of methionine residues. False discovery rate (FDR) was set at 0.01, both at the peptide and protein level. Only proteins identified with at least 2 peptides were considered. Protein intensities, as calculated by the software, were used to highlight significant differences between groups (p-value ≤ 0.001, Supplementary Table 1).

TMT-labelled peptides were separated under the same conditions specified above but using a linear gradient of ACN from 3 % to 50 % in 90 min and a different acquisition method. A full MS scan in the range 300–1700 *m/z* in the Orbitrap (30,000 nominal resolution) was followed by three MS/MS scans acquired both in the linear trap (CID fragmentation for identification purposes) and in the Orbitrap (HCD fragmentation, 7500 nominal resolution, for quantification purposes). All

peptides identified with high confidence (as detailed below) were used to generate a static exclusion list and samples were analyzed a second time under identical chromatographic and instrumental conditions but for the application of the exclusion list.

Raw files were analyzed with the software package Proteome Discoverer (version 1.4, Thermo Fisher Scientific) interfaced to a Mascot search engine (version 2.2.4, Matrix Science) against the same database specified above. A MudPIT protocol was applied with the following search parameters: trypsin as digesting enzyme with up to 2 missed cleavages allowed; 10 ppm and 0.6 Da for peptide and fragment tolerance, respectively; carbamidomethylation of cysteines and TMT-6plex (*N*-term and K) were set as fixed modifications, while methionine oxidation as variable modification. The algorithm Percolator was used to assess the FDR which was set at 0.01 both for peptides and proteins. Only proteins identified with at least 2 unique peptides were further considered. TMT reporter ion intensities were used to quantify proteins and highlight significant differences between groups (p-value ≤ 0.001, Supplementary Table 2).

3.4. Targeted proteomic analysis

The targeted proteomic analysis was carried out by LC-MS/MS using a triple quadrupole (TSQ Quantiva, Thermo Fisher Scientific, USA) coupled to a UHPLC Ultimate 3000 (Dionex - Thermo Fisher Scientific, USA), on the asymptomatic and symptomatic individual samples used to prepare pools in the untargeted proteomic analysis.

Peptides were separated by reverse-phase chromatography with a C18 column (Brownlee SPP Peptide ES C18, 100 mm × 2.1 mm i.d., 2.7 μm particle size, Perkin Elmer), maintained at 30 °C. Peptides separation occurred with a 45 min gradient, using 0.1 % formic acid in aqueous solution (A) and 0.1 % formic acid in acetonitrile (B) as mobile phases. The gradient started at 2.5 % B and increased up to 50 % B in 34 min. Flow rate was set to 0.200 mL/min and the injection volume was 11 μL. Two technical replicates were acquired for each sample. The mass spectrometer operated in selected reaction monitoring (SRM) mode, with the following parameters: positive ionization mode, spray voltage at 3000 V, ion transfer tube and vaporizer temperature at 325 °C, CID argon pressure at 1.5 mTorr, sheath gas 25 (Arb), auxiliary gas 10 (Arb), sweep gas 0 (Arb), Q1 and Q3 resolution 0.7 (FWMH). Proteotypic peptides of selected proteins were predicted with Skyline MS software v. 21.1 [21] and shortlisted when necessary, giving priority to the peptides that were actually identified in the untargeted analysis. The SRM transitions were downloaded from SRMAtlas database [22] and experimentally optimized. The complete list of optimized transitions is reported in Supplementary Table 3.

Raw MS data were analyzed with Skyline and a relative quantification between A and S patients was obtained comparing the average area of the most intense transition for each monitored peptide.

3.5. Bioinformatic and statistical analysis

To highlight physical/functional interactions between proteins identified by the untargeted proteomic analyses and enriched pathways and biological functions the tools STRING [23], g:GOST of g:Profiler [24] and Revigo [25] were used. All other analyses were performed using R for statistical computing (R Foundation for Statistical Computing, Vienna, Austria). Since peptide levels were highly skewed, data were firstly scaled and centered before analyses. Visual correlation matrix was used for identifying associations between variables, using the complete clustering as agglomeration method. Two dimensional and three-dimensional principal component analyses (PCA) were performed using the function "PCA", with ggplot as a graphical engine. Heatmap analysis was performed using "canberra" as distance function and "Ward.D2" as clustering method of the R function "heatmap". Logistic regression was performed using groups as class independent variables and scaled peptides levels as covariates.

4. Results

Table 2 reports the demographical and clinical features of the controls, asymptomatic and symptomatic subjects.

In order to identify disease associated salivary peptides/proteins, in the first stage of the study, four or five individual saliva samples from each study group were randomly selected and pooled using an isovolumetric strategy (Table 1).

Endogenous peptides, derived from the spontaneous or protease-dependent degradation of saliva proteins, were isolated by filtration with a 10 kDa membrane, as described in the methods section. An untargeted label-free LC-MS/MS approach was applied to compare the abundance of peptides in the four saliva pools obtained for each study group. LC-MS/MS analyses were performed in technical duplicate, i.e. each sample was analyzed twice, under the same instrumental and chromatographic conditions. A high correlation was found between the signal intensities obtained from the duplicated measurements of each pool (mean correlation: r = 0.99 for Control, r = 0.98 for Asymptomatic and r = 0.99 for Symptomatic), thus showing that results were technically sound and highly reproducible.

Raw data files were analyzed with the software MaxQuant interfaced to the Andromeda search engine, using an unrestricted search setting (no enzyme). Identified peptides were referred to their original proteins when at least two unique peptides were identified with high confidence (FDR $\leq$ 0.01). Using this approach, a total of 53 proteins were identified, their fold changes and statistical significance being reported in Supplementary Table 1. Two proteins characterized SARS-CoV-2 infection: 1) Actin-depolymerizing factor (ADF) detected in controls but not in infected subjects, and 2) Interleukin-1 receptor antagonist protein (IL1RA), which had an opposite behavior, i.e. absent in controls but present in infected subjects. For the majority of proteins, no significant differences were found between asymptomatic and symptomatic groups, with some highly significant exceptions, including basic salivary proline-rich proteins (PRPs), desmocollin-2 (DSC2), fatty acid binding protein 5 (FABP5), histatin 1 (his-1), salivary acidic proline rich phosphoprotein ½ (PRH1), statherin (STATH), submaxillary gland androgen regulated protein 3B (SMR3B), annexin A1 (ANXA1), mucin 7 (MUC7), alpha-actinin-4 (ACTN4), immunoglobulin kappa variable 1–33 (IGKV1-33), protein-glutamine gamma-glutamyltransferase E (TGM3) and the collagen alpha 1(VIII) chain (COL8A1) (Supplementary Table 1).

The same saliva pools, obtained as described above, were then subjected to a label-based quantitative proteomic approach (Tandem Mass Tags, TMT) to identify salivary proteins with different abundance between groups. After removal of the endogenous peptides, proteins were reduced, alkylated and trypsin digested using a filter aided sample preparation protocol (FASP), as detailed in the methods section. Tryptic peptides from the different pools were then labeled with TMT reagents and mixed. LC-MS/MS analysis and protein identification and quantification was performed as described in the methods section. A total of 117 proteins were identified and quantified (Supplementary Table 2). The abundance of six proteins (BPI fold-containing family A member 2, Histone H3 (Fragment), Histone H4, Integrin alpha-M, Small proline-rich protein 3 (Fragment), Keratin, type II cytoskeletal 1) was lower among SARS-CoV-2 positive subjects with respect to controls, while the opposite pattern was observed for another series of four proteins (Galectin-3-binding protein, Immunoglobulin J chain (Fragment), Interleukin-1 receptor antagonist protein, Polymeric immunoglobulin receptor). For 80 of the 117 proteins reported in Supplementary Table 2, significant differences in abundance levels were found between asymptomatic and symptomatic SARS-CoV-2 subjects, 11 proteins showing a fold change (FC) 2, or ≤ -2 (Table 3).

We then focused on infected subjects to search biomarkers of disease severity. First the 80 significantly differentially abundant proteins between asymptomatic and symptomatic subjects were selected to perform a String Network Analysis [23] and g:GOST functional profiling [24]. The String Network Analysis highlights how these 80 proteins are physically/functionally highly interconnected (Fig. 1), and g:GOST functional profiling, allowed the identification of 12 highly enriched significant pathways, mainly encompassing the host response to infection (Fig. 2).

The 117 proteins identified by the label-based approach were then compared to the 53 proteins identified with the analysis of endogenous

Table 2

Demographic and clinical features of the studied subjects, including control, asymptomatic and symptomatic SARS-CoV-2 positive subjects.

	Control n = 20	Asymptomatic n = 19	Symptomatic n = 16	p-value[#]
Age, (mean ± SD, yrs)	47.0 ± 16.1	44.6 ± 14.6	62.2 ± 20.0*	**0.007**
Gender, n F/M (%F)	12/8 (60 %)	7/12 (37 %)	5/11 (31 %)	0.199
Pneumonia, n (%)	–	0 (0.0 %)	8 (50.0 %)	**<0.001**
Fever, n (%)	–	7 (36.8 %)	12 (75.0 %)	**0.027**
Anosmia, n (%)	–	3 (15.8 %)	0 (0.0 %)	0.148
Ageusia, n (%)	–	1 (5.3 %)	0 (0.0 %)	0.543
Asthenia, n (%)	–	4 (21.1 %)	1 (6.3 %)	0.347
Cough, n (%)	–	4 (21.1 %)	4 (25.0 %)	0.548
Headache, n (%)	–	1 (5.3 %)	1 (6.3 %)	0.713
GI, n (%)	–	0 (0.0 %)	5 (31.3 %)	**0.013**
Arthralgia, n (%)	–	1 (5.3 %)	2 (12.5 %)	0.434
Myalgia, n (%)	–	2 (10.5 %)	1 (6.3 %)	0.566
Dyspnea, n (%)	–	2 (10.5 %)	4 (25.0 %)	0.379
Rhinitis, n (%)	–	5 (26.3 %)	0 (0.0 %)	**0.036**
Nausea, n (%)	–	0 (0.0 %)	0 (0.0 %)	1.000
Pharyngodynia, n (%)	–	0 (0.0 %)	3 (18.8 %)	0.086

GI: Gastrointestinal symptoms. [#]Statistical analysis was made by One-way Anova for age, and by the Chi-square test for all the remaining variables. *Bonferroni's test for pairwise comparisons: p < 0.05 with respect to Control and Asymptomatic subjects. Significant p-values are in bold.

Table 3

Significantly differentially abundant proteins between Symptomatic (S) and Asymptomatic (A) groups. Only proteins with a Fold Change (FC) ≥ 2 or ≤ -2 are reported. For comparison, the pattern of any protein in S and A groups with respect to Controls (C) is reported as FC, which might be non significant (ns) or significant (*).

Protein ID	Description	Gene Name	FC		
			S/A	S/C	A/C
P31949	Protein S100-A11	S100A11	−2.55	1.17 ns	3.18*
Q6P5S2	Protein LEG1 homolog	LEG1	−2.54	−1.48 ns	1.37 ns
P05109	Protein S100-A8	S100A8	−2.51	−1.29 ns	2.06*
F8VV32	1,4-beta-*N*-acetylmuramidase C	LYZ	−2.35	−1.03 ns	3.21*
A0A0A0MS51	Actin-depolymerizing factor	GSN	−2.15	1.45 ns	2.96*
Q02413	Desmoglein-1	DSG1	−2.13	−1.27 ns	1.67 ns
A8K2U0	Alpha-2-macroglobulin-like protein 1	A2ML1	−2.00	1.17 ns	2.39*
P01876	Immunoglobulin heavy constant alpha 1	IGHA1	−2.00	1.32 ns	2.44*
B9A064	Immunoglobulin lambda-like polypeptide 5	IGLL5	−2.04	1.65 ns	3.46*
P09228	Cystatin-SA	CST2	2.24	1.17 ns	−1.22 ns
P23280	Carbonic anhydrase 6	CA6	2.51	−1.46 ns	−2.91*

Fig. 1. String Network Analysis of the proteins identified as significantly different between asymptomatic and symptomatic groups. Lines connecting the different nodes represent functional and/or physical interactions. Red and blue nodes represent proteins involved in the immune system and in the innate immune system, respectively.

peptides; this allowed the identification of a total of 26 common proteins (Supplementary Table 4).

To validate the results obtained with saliva pools and rule out possible biases due to the way the different patient samples were mixed, a LC-MS/MS Selected Reaction Monitoring (SRM) analysis was performed on all individual patient samples using a triple quadrupole mass spectrometer interfaced to an HUPLC system, as detailed in the methods section. This targeted approach was carried out on a subset of the most interesting proteins identified with the untargeted proteomic approaches described above. In particular, the following ten proteins were selected among the 26 commonly identified by the label-free peptidome analysis and the label-based proteome analysis (Supplementary Table 4): IL1RA, S100A8, S100A9, CRNN (Cornulin), CYST-SA, CYSTB, CA6, GAPDH (G3PD), FABP5, DSC2. These proteins were considered as the most relevant based on the data obtained from the untargeted approaches and on the scrutiny of the literature, for their involvement in the processes of inflammation, metabolism and cellular adhesion. Proteins were first trypsin digested and the abundance of the derived

proteotypic peptides were monitored by a LC-MS/MS-SRM method. For each protein 3 to 4 proteotypic peptides were selected (with the exception of DSC2 protein for which only 2 peptides were considered) and for each peptide 4 different transitions were monitored. The complete list of optimized transitions is reported in Supplementary Table 3. Two technical replicates were collected for each sample. For each peptide the most intense transition was used for quantification. Duplicate data were averaged, and a final data matrix was built for the subsequent statistical analysis, which always included age as covariate.

Peptide data were highly skewed. Each peptide level was log10 transformed and results are shown in Fig. 3. Data were then scaled and centered before bioinformatic analyses. Age was included in the analyses.

Fig. 4 shows the hierarchical clustered correlation matrix, which indicates that, as expected, peptides derived from the same protein cluster together. The most significant correlations between peptides were reported in red (positive) and violet (negative). Inverse correlations between S100A8/S100A9 and carbonic anhydrase 6 are clearly

Fig. 2. Manhattan plot reporting the enrichment analysis of GO terms associated to the proteins identified as differently abundant in asymptomatic and symptomatic groups. The top twelve most significant GO-terms are listed.

ID	Source	Term ID	Term Name	p_{adj} (query_1)
1	GO:MF	GO:0061134	peptidase regulator activity	8.612×10^{-11}
2	GO:BP	GO:0006959	humoral immune response	5.591×10^{-15}
3	GO:BP	GO:0042742	defense response to bacterium	6.391×10^{-14}
4	GO:BP	GO:0052547	regulation of peptidase activity	1.525×10^{-13}
5	GO:BP	GO:0044419	biological process involved in interspecies interact…	6.581×10^{-13}
6	GO:BP	GO:0006950	response to stress	4.557×10^{-12}
7	GO:BP	GO:0051707	response to other organism	2.463×10^{-10}
8	GO:CC	GO:0005576	extracellular region	1.353×10^{-48}
9	GO:CC	GO:0099503	secretory vesicle	5.143×10^{-26}
10	REAC	REAC:R-HSA-67…	Neutrophil degranulation	1.081×10^{-16}
11	REAC	REAC:R-HSA-16…	Innate Immune System	7.209×10^{-14}
12	GO:CC	GO:0031410	cytoplasmic vesicle	1.026×10^{-16}

depicted in Fig. 4 (violet area, bottom right).

Principal component analysis (PCA) was used to evaluate whether the asymptomatic and symptomatic groups could be differentiated by peptides abundances (Fig. 5). The first dimension of PCA (panel A) was mainly explained by IL1RA and CYSTB; the second dimension (panel B) was associated mainly to S100A8 and S100A9. The bidimensional plot after PCA with superimposed ellipses (which contain approximately 95 % of data) shows that groups partially overlap (panel C). A further analysis, made by a tridimensional plot (panel D), resulted in a better discrimination between groups. Panel E shows that the third dimension is mainly associated to CA6, age and FABP5.

A further analysis was made by means of heatmaps using Canberra distances and Ward clustering (Fig. 6). The results obtained showed two main clusters of subjects, each of which could be further divided into two subgroups. The horizontal clustering shows that asymptomatic (A) and symptomatic (S) subjects presented heterogeneous levels of peptides. However, within the first sub-clustered group, the further division identified asymptomatic (A) and symptomatic (S) subjects more homogenously. The vertical clustering shows that peptides are correctly clustered together.

Due to the effective discrimination between asymptomatic and symptomatic groups obtained with the heatmap, a series of univariate logistic regressions analyses were performed using the groups as outcome, and peptides as explanatory variables. P-values were adjusted for multiple comparisons by the Benjamini-Hochberg procedure. Results reported in Table 4, show that significant association to symptomatic COVID-19 were obtainable for peptides derived from S100A8, S100A9, CYST-SA and CA6, whereas the covariate variable age was not significantly associated to SARS-CoV-2 presence or absence of symptoms.

To evaluate whether the studied proteins were correlated with the disease severity, we considered the group of symptomatic patients (S). In this group clinical (age, gender, pneumonia, time from onset), hematological and biochemical data (reported in Supplementary Table 5) were correlated with the abundance of any peptide monitored by LC-MS/MS-SRM as reported in Table 4. Peptide abundances do not correlate with clinical and biochemical data, while hematological data correlated with the estimated abundance of two proteins, CA6 and S100A8. Platelets count correlated with CA6 ($r = 0.5324$, $p = 0.0338$; $r = 0.4706$, $p = 0.0658$; $r = 0.5794$, $p = 0.0187$ for the three analyzed peptides sequentially reported in Table 4). S100A8 correlated with lymphocytes ($r = 0.5147$, $p = 0.0413$; $r = 0.4618$, $p = 0.0718$; $r = 0.4706$, $p = 0.0658$), and monocytes count ($r = 0.4492$, $p = 0.0809$; $r = 0.5552$, $p = 0.0256$; $r = 0.4374$, $p = 0.0902$). S100A9 behaved similarly to S100A8, although correlations did not reach statistical significance.
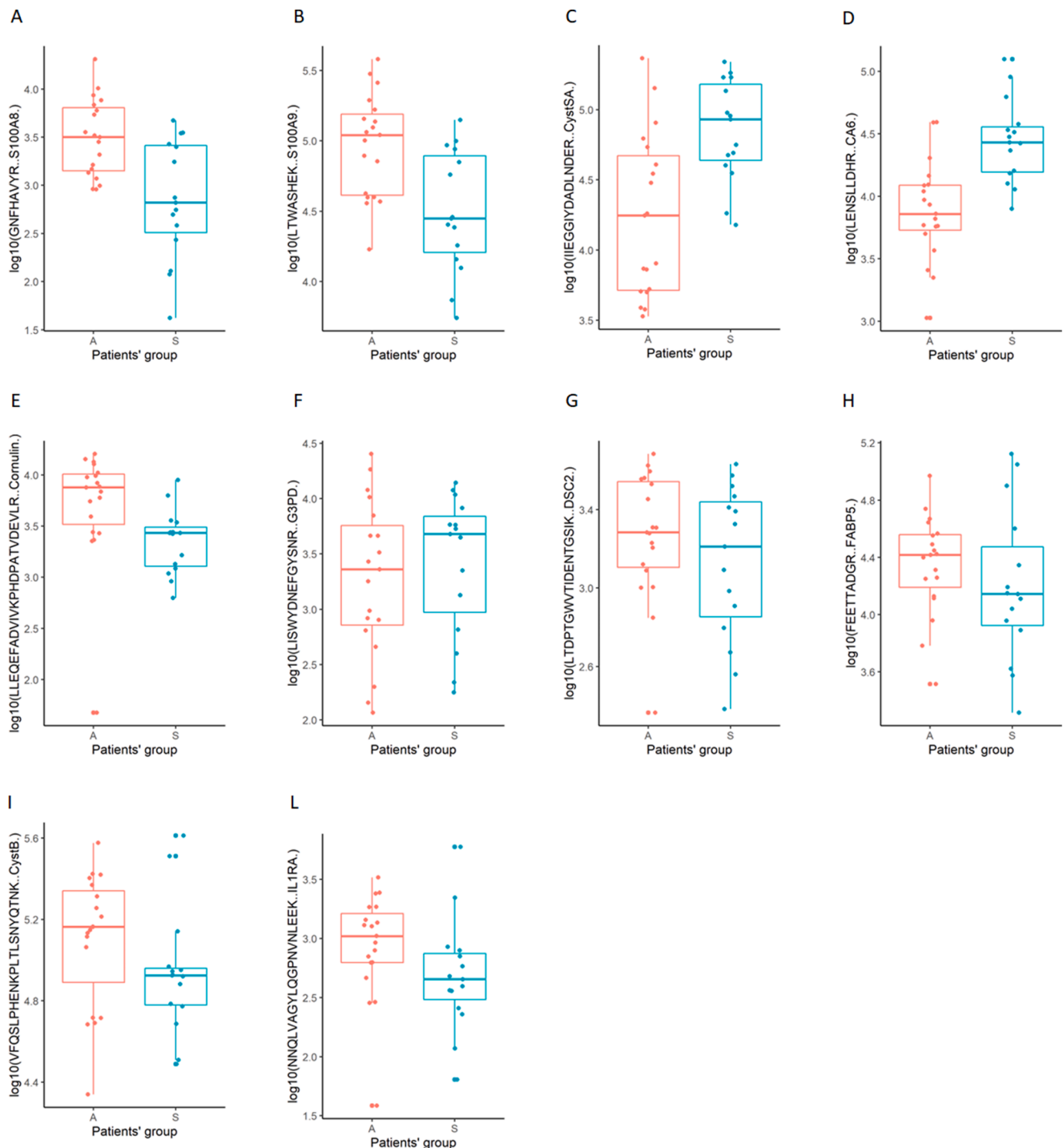
Fig. 3. Boxplots with individual data points (dots) of $\log_{10}$ transformed peptide levels, subdivided by patients' groups (A = Asymptomatic and S = Symptomatic).

5. Discussion and conclusions

The present study was undertaken to identify new potential salivary biomarkers of COVID-19 disease. Saliva was chosen because SARS-CoV-2 is reported to infect salivary glands which, in turn, might become a reservoir for the virus [26,27]. Being non-invasive, saliva collection is tolerated by patients more than sera collection; moreover, this biofluid requires less pre-analytical handling before proteomic analysis since it is less enriched than plasma in abundant proteins, such as albumin [28]. The clinical spectrum of SARS-CoV-2 infection ranges from the complete absence of symptoms to severe disease. The outcome of the infection is unpredictable, although more severe disease is reported mainly among older subjects and immunocompromised patients [5,7]. We retrospectively selected and compared saliva samples obtained from controls and two groups of SARS-CoV-2 positive subjects: asymptomatic (group A) and inpatients with COVID-19 disease (symptomatic group-S). In order to minimize potential comparison bias between the two SARS-CoV-2 groups, they shared the: 1) enrollment period and geographic area to limit SARS-CoV-2 variant-related differences; 2) Ct values of molecular testing to avoid extremes with very high (Ct < 20) or very low (Ct > 30) viral loads; 3) absence of any previous vaccination since they were enrolled before the beginning of the vaccine campaign.
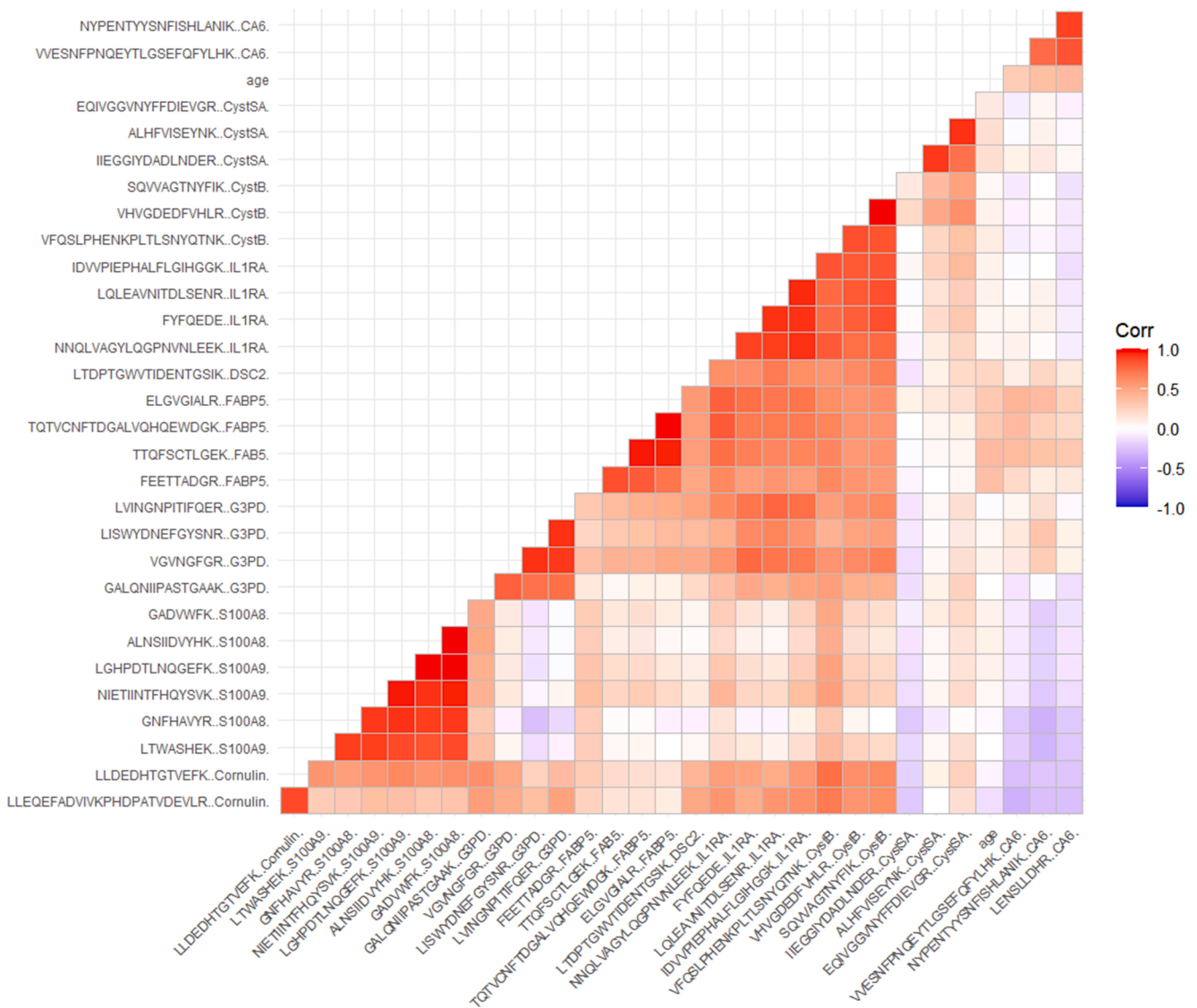
Fig. 4. Hierarchical clustered correlation matrix of all studied peptides, including age.

A potential bias and limitation of our study might depend on the differences between asymptomatic and symptomatic groups in the duration of infection, which could not be determined for asymptomatic subjects. Moreover, another potential limitation might be represented by a previous history of oral condition that would affect the composition of saliva. In order to make the proteomic analysis as comprehensive as possible, both the intact protein fraction and the endogenous peptides fraction were analyzed. Peptides in saliva might result from post-collection proteolytic degradation, but they might also be representative of oral physiology as described for PRPs deriving from the pre- and post-secretion proteolytic processing of the basic and acidic Proline-Rich Proteins. PRPs might exert anti-microbial but also detoxifying effects [29]. PRPs were significantly lower in both asymptomatic and symptomatic SARS-CoV-2 subjects with respect to controls, the reduction being more pronounced in the asymptomatic than in the symptomatic group subjects (Supplementary Table 1). This finding suggests that PRPs might be involved in the host defense to SARS-CoV-2 orally, possibly contributing to limiting viral spread. A similar pattern was observed for peptides derived from the most abundant salivary proteins (i.e., basic and acidic Proline-Rich Proteins, statherin, and histatin-1).

On the contrary, Desmocollin-2 (DSC2), Fatty acid-binding protein 5 (FABP5) and Interleukin-1 receptor antagonist protein (IL1RA) derived peptides tended to increase mainly in asymptomatic subjects with respect to controls, and this was associated with a significant reduction in abundance among symptomatic subjects as compared to the asymptomatic ones. DSC2 members of the cadherin superfamily mediate adhesion to desmosomes [20,30], and currently no data are present in the literature regarding its role in COVID-19. FABP5 is involved in long chain fatty acid intracellular transport, being able to bind linoleic acid (LA) [20]. Interestingly, it has been recently reported that SARS-CoV-2 spike (S) glycoprotein has a receptor-binding domain that tightly binds LA in three composite binding pockets. This binding stabilizes a locked S conformation, resulting in a reduction in both angiotensin-converting enzyme 2 (ACE2) interaction *in vitro* and SARS-CoV-2 replication [31]. The significantly reduced levels of FABP5 peptides among symptomatic patients was correlated with increased levels of the intact protein, suggesting that a reduced fragmentation of the protein might reduce free LA availability in the mouth, thus favoring the unlocked S protein conformation and ACE2 receptor binding and dissemination. IL1RA peptides and protein were reduced in symptomatic patients, in line with the effect of this antagonist on IL1, a cytokine that is primarily involved in COVID-19 pathogenesis [32]. Any absence of a counterbalance might favor inflammation and disease.

The label-based proteomic analysis showed that many of the differentially abundant proteins between A and S groups were mainly representative of the innate immune response to infections (Figs. 1 and 2).
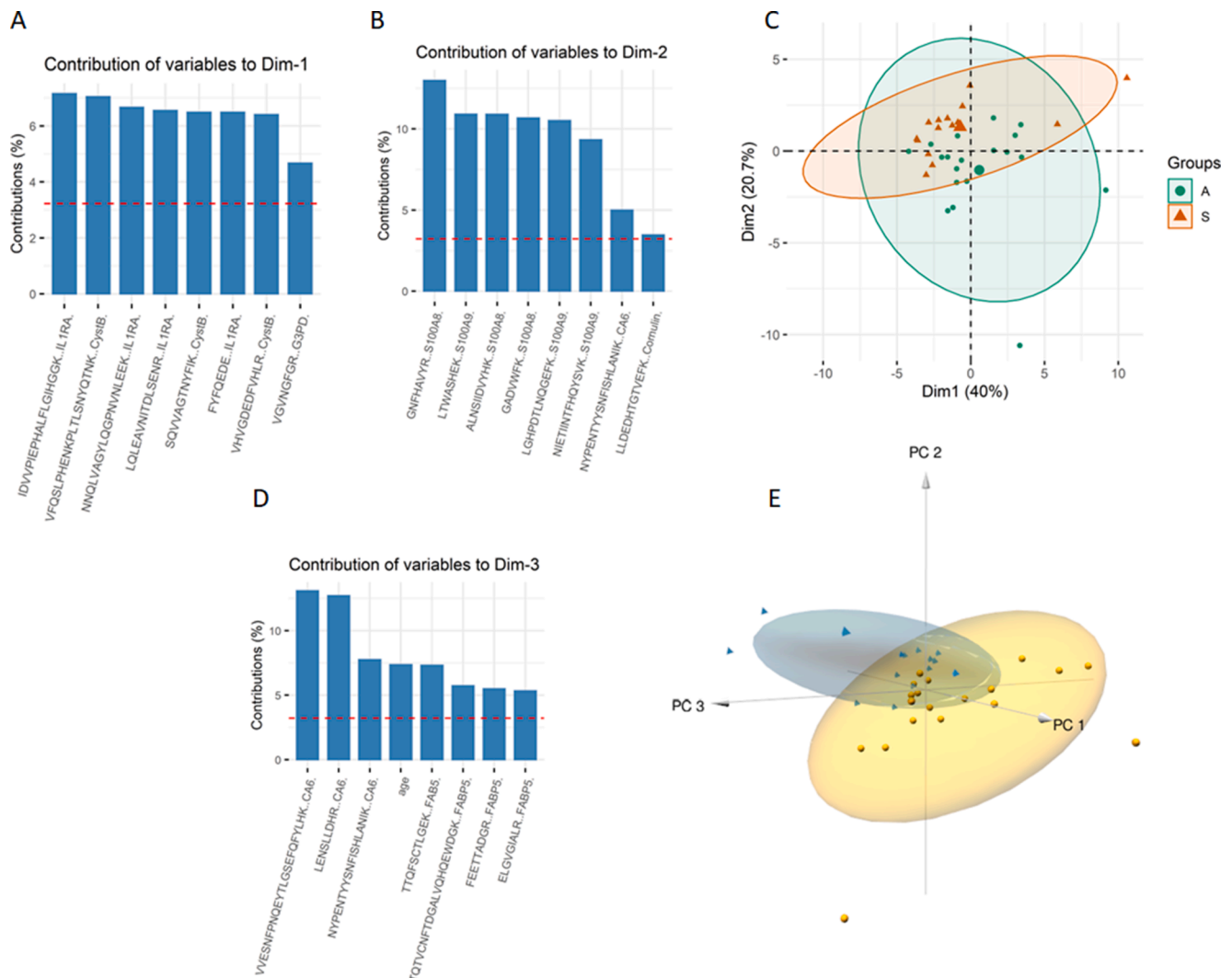
Fig. 5. Principal Component Analysis (PCA) results, obtained using scaled data of all the studied proteotypic peptides and patients' age. Panels A and B report the contribution of the 8 most important variables in explaining Dimensions 1 and 2, respectively. Panel C reports the bidimensional plot of PCA, with individual patients divided by asymptomatic (A) and symptomatic (S) and with superimposed the two ellipsoids (each including 95% of individuals); Panel D reports the contribution of the 8 most important variables in explaining Dimensions 3. Panel E shows the three-dimensional plot of PCA, with the superimposed the two ellipsoids.

These are generally significantly lower in the symptomatic patients as compared to the asymptomatic subjects. This finding suggests that SARS-CoV-2 evolving towards a more severe disease is probably due, at least in part, not only to an impaired systemic innate immunity but also to an impaired innate immunity at the portal entry of the virus: the mouth. Of the innate immunity proteins belonging to the S100 family, S100A11 significantly increased in asymptomatic, but not in symptomatic subjects with respect to controls and a similar, although less significant pattern, was observed for S100A8 and S100A9. Increased levels of these calcium binding proteins were also found in asymptomatic with respect to symptomatic patients. To explain the discrepancy between this finding and data previously collected on serum [33–35] it is important to consider the complexity of S100 biology: these proteins might have opposite effects (e.g., pro- or anti-inflammatory) depending on the target tissue or organ and on the cellular status [36]. It is therefore possible that at the systemic level they might amplify the inflammatory response with severe clinical consequences, while at the oral mucosa they might induce an inflammatory reaction able to limit viral spread.

Two proteins, Carbonic anhydrase 6 (CA6) and Cystatin-SA (CYST-SA), were highly expressed by COVID-19 symptomatic inpatients with respect to asymptomatic subjects, although both were reduced with

respect to controls, in agreement with the recent findings from Munoz-Prieto et al. [37]. Both proteins are involved in taste perception [20,38,39]. These findings are in line with the SARS-CoV-2 correlated ageusia, although in our series this clinical manifestation was extremely rare. From the untargeted peptidomic and proteomic analyses two further proteins are worth mentioning: Alpha-actinin-4 and actin depolymerization factor. Both proteins were reduced in symptomatic COVID-19 patients and both are involved in cytoskeletal remodeling, cell motility but also in virus entry into the host cells [40].

Proteomic and peptidomic results discussed so far were obtained from analyses of pooled samples. To validate our results, a representative series of the most interesting proteins identified with the untargeted approaches was quantified in single samples by LC-MS/MS-SRM approach. No significant variations could be found for Glyceraldehyde-3-phosphate dehydrogenase (G3PD), while CYST-SA and CA6 have a significantly increased abundance in symptomatic with respect to asymptomatic subjects. All these results confirmed those obtained with the untargeted approach using saliva pools. Differences in CA6 and CYST-SA expression in COVID-19 patients with respect to a control group were recently reported also by Munoz-Prieto et al. [37], thus suggesting that the dysregulation of CA6 and CYST-SA can result in taste and smell perception perturbation caused by COVID-19.

Fig. 6. Hierarchical clustered heatmap analysis, performed including peptides, age and patients' groups.

The results obtained by the quantification of FABP5 deserve consideration, since a wide data distribution was observed, with median levels that tended to be lower among symptomatic than asymptomatic subjects; this finding is not in line with the increased levels found by the untargeted proteomic analysis, but it is in line with the findings of the untargeted peptidomic analysis. We might hypothesize that an increased fragmentation of FABP5 might occur in symptomatic subjects causing reduced levels of the intact protein as detected by targeted SRM analysis. Furthermore, this discrepancy might also depend on the differences

between the two analytical approaches: untargeted peptidomic and proteomic analyses were performed on pooled saliva samples, while individual samples were analyzed by the targeted SRM approach. Therefore, the differences observed when pools were analyzed might be due to the high levels present in some patients, which affect the overall levels of the pooled samples.

PCA and hierarchical clustering were performed to identify potential diagnostic clusters of proteins able to distinguish between asymptomatic and symptomatic subjects. First and second PCA dimensions did not

Table 4
Univariate logistic regression analyses. Asymptomatic and Symptomatic groups were outcome variables, LC-MS/MS-SRM peptides were explanatory variables and age was covariate. P-values and Benjamini & Hochberg adjusted (BH) p-values were reported.

Protein	Peptide name (included in the model)	Coefficients	unadjusted p-value	BH p-value
IL1RA	NNQLVAGYLQGPNVNLEEK.IL1RA	0.126	0.126	0.245
	LQLEAVNITDLSENR.IL1RA	0.381	0.381	0.493
	IDVVPIEPHALFLGIHGGK.IL1RA	0.314	0.314	0.438
	FYFQEDE.IL1RA	0.313	0.313	0.438
Cornulin	LLEQEFADVIVKPHDPATVDEVLR.Cornulin	0.053	0.053	0.109
	GQNRPGVQTGGQATGSAWVSSYDR.Cornulin	0.019	0.019	0.052
	LLDEDHTGTVEFK.Cornulin	0.026	0.026	0.063
CA6	VVESNFPNQEYTLGSEFQFYLHK.CA6	0.004	**0.004**	**0.041**
	NYPENTYYSNFISHLANIK.CA6	0.006	**0.006**	**0.041**
	LENSLLDHR.CA6	0.004	**0.004**	**0.041**
FABP5	TQTVCNFTDGALVQHQEWDGK.FABP5	0.913	0.913	0.913
	TTQFSCTLGEK.FABP5	0.894	0.894	0.913
	ELGVGIALR.FABP5	0.730	0.730	0.838
	FEETTADGR.FABP5	0.325	0.325	0.438
CYST-SA	IIEGGIYDADLNDER.CYST-SA	0.006	**0.006**	**0.041**
	ALHFVISEYNK. CYST-SA.	0.016	**0.016**	0.052
	EQIVGGVNYFFDIEVGR. CYST-SA	0.036	**0.036**	0.080
S100A8	ALNSIIDVYHK.S100A8	0.015	**0.015**	0.052
	GNFHAVYR.S100A8	0.008	**0.008**	**0.041**
	GADVWFK.S100A8	0.017	**0.017**	0.052
DSC2	LTDPTGWVTIDENTGSIK.DSC2	0.269	0.269	0.416
CYSTB	VHVGDEDFVHLR.CYSTB	0.202	0.202	0.329
	SQVVAGTNYFIK. CYSTB	0.154	0.154	0.266
	VFQSLPHENKPLTLSNYQTNK. CYSTB	0.144	0.144	0.262
G3PD	LISWYDNEFGYSNR.G3PD	0.546	0.546	0.651
	VGVNGFGR.G3PD	0.862	0.862	0.913
	LVINGNPITIFQER.G3PD	0.788	0.788	0.873
	GALQNIIPASTGAAK.G3PD	0.413	0.413	0.513
S100A9	LGHPDTLNQGEFK.S100A9	0.020	**0.020**	0.052
	LTWASHEK.S100A9	0.008	**0.008**	**0.041**
	NIETIINTFHQYSVK.S100A9	0.014	**0.014**	0.052

Significant p-values are in bold.

enable a distinction between the two groups since the two ellipsoids overlapped. However, a clearer distinction between groups was achieved with third dimension PCA. In this analysis, major determinants were age, CA6 and FABP5. Hierarchical clustering clearly showed the prevalence of reduced protein levels distinguishing between asymptomatic and symptomatic subjects. Four main protein clusters emerged: 1) S100A8 and S100A9; 2) CYST-SA and CA6; 3) DSC2 and FABP5; 4) CYSTB, Cornulin, IL1RA and G3PD. On the other hand, two main patient arms were clustered, each cluster further comprising two subgroups. Protein clusters 1 and 4 were associated with asymptomatic group whereas protein clusters 2 and 3 were associated with symptomatic group. At logistic regression analysis, proteins significantly correlated with group S were CA6, S100A8, S100A9 and CYST-SA. Notably CA6 and S100A8 variations in this group of patients were correlated with thrombocytopenia and lymphopenia, two well-known hallmarks of SARS-CoV-2 infection [41].

In conclusion, our findings suggest that salivary proteins are not only associated with SARS-CoV-2 infection but might also be a valid tool in detecting the presence of a more severe disease form. Due to their significance in pathogenesis, the differentially abundant proteins involved in innate immunity (e.g., S100 proteins), in taste (e.g., CA6 and cystatins), and those potentially involved in modifying viral binding to the host receptor (e.g., FABP5), appear to be of interest for use as potential biomarkers, and as possible targets for the development of new drugs.

Declaration of Competing Interest

The authors declare that they have no known competing financial interests or personal relationships that could have appeared to influence the work reported in this paper.

Data availability

Data will be made available on request.

Appendix A. Supplementary data

Supplementary data to this article can be found online at https://doi.org/10.1016/j.cca.2022.09.023.

References

[1] J.-W. Chan, S. Yuan, K.-H. Kok, K.-W. To, H. Chu, J. Yang, F. Xing, J. Liu, C.-Y. Yip, R.-S. Poon, H.-W. Tsoi, S.-F. Lo, K.-H. Chan, V.-M. Poon, W.-M. Chan, J.D. Ip, J.-P. Cai, V.-C. Cheng, H. Chen, C.-M. Hui, K.-Y. Yuen, A familial cluster of pneumonia associated with the 2019 novel coronavirus indicating person-to-person transmission: a study of a family cluster, The Lancet 395 (10223) (2020) 514–523.

[2] A. Lee, Wuhan novel coronavirus (COVID-19): why global control is challenging? Public Health 179 (2020) A1–A2.

[3] Z. Wu, J.M. McGoogan, Characteristics of and important lessons from the coronavirus disease 2019 (COVID-19) outbreak in China: summary of a report of 72 314 cases from the Chinese Center for Disease Control and Prevention, JAMA 323 (13) (2020) 1239–1242.

[4] J. He, Y. Guo, R. Mao, J. Zhang, Proportion of asymptomatic coronavirus disease 2019: a systematic review and meta-analysis, J. Med. Virol. 93 (2) (2021) 820–830.

[5] S. Richardson, J.S. Hirsch, M. Narasimhan, J.M. Crawford, T. McGinn, K. W. Davidson, D.P. Barnaby, L.B. Becker, J.D. Chelico, S.L. Cohen, J. Cookingham, K. Coppa, M.A. Diefenbach, A.J. Dominello, J. Duer-Hefele, L. Falzon, J. Gitlin, N. Hajizadeh, T.G. Harvin, D.A. Hirschwerk, E.J. Kim, Z.M. Kozel, L.M. Marrast, J. N. Mogavero, G.A. Osorio, M. Qiu, T.P. Zanos, Presenting characteristics, comorbidities, and outcomes among 5700 patients hospitalized with COVID-19 in the New York City area, JAMA 323 (20) (2020) 2052.

[6] W.-J. Guan, Z.-y. Ni, Y.u. Hu, W.-H. Liang, C.-Q. Ou, J.-X. He, L. Liu, H. Shan, C.-L. Lei, D.S.C. Hui, B. Du, L.-J. Li, G. Zeng, K.-Y. Yuen, R.-C. Chen, C.-l. Tang, T. Wang, P.-Y. Chen, J. Xiang, S.-Y. Li, J.-L. Wang, Z.-J. Liang, Y.-X. Peng, L.i. Wei, Y. Liu, Y.-H. Hu, P. Peng, J.-M. Wang, J.-Y. Liu, Z. Chen, G. Li, Z.-J. Zheng, S.-Q. Qiu, J. Luo, C.-J. Ye, S.-Y. Zhu, N.-S. Zhong, China medical treatment expert group for Covid-19, clinical characteristics of coronavirus disease 2019 in China, N. Engl. J. Med. 382 (18) (2020) 1708–1720.

[7] C. Huang, Y. Wang, X. Li, L. Ren, J. Zhao, Y.i. Hu, L.i. Zhang, G. Fan, J. Xu, X. Gu, Z. Cheng, T. Yu, J. Xia, Y. Wei, W. Wu, X. Xie, W. Yin, H. Li, M. Liu, Y. Xiao, H. Gao, L.i. Guo, J. Xie, G. Wang, R. Jiang, Z. Gao, Q.i. Jin, J. Wang, B. Cao, Clinical features of patients infected with 2019 novel coronavirus in Wuhan, China, The Lancet 395 (10223) (2020) 497–506.

[8] D.J. Smith, A.J. Hakim, G.M. Leung, W. Xu, W.W. Schluter, R.T. Novak, B. Marston, B.S. Hersh, COVID-19 mortality and vaccine coverage — Hong Kong Special Administrative Region, China, January 6, 2022–March 21, 2022, MMWR Morb. Mortal. Wkly. Rep. 71 (15) (2022) 545–548.

[9] Y. Li, Y. Wang, H. Liu, W. Sun, B. Ding, Y. Zhao, P. Chen, L. Zhu, Z. Li, N. Li, L. Chang, H. Wang, C. Bai, P. Xu, Urine proteome of COVID-19 patients, URINE 2 (2020) 1–8.

[10] D.-G. Mun, P.M. Vanderboom, A.K. Madugundu, K. Garapati, S. Chavan, J.A. Peterson, M. Saraswat, A. Pandey, DIA-based proteome profiling of nasopharyngeal swabs from COVID-19 patients, J. Proteome Res. 20 (8) (2021) 4165–4175.

[11] A. Alaiya, A. Alshukairi, Z. Shinwari, M. Al-Fares, J. Alotaibi, W. AlOmaim, et al., Alterations in the plasma proteome induced by SARS-CoV-2 and MERS-CoV reveal biomarkers for disease outcomes for COVID-19 patients, J. Inflamm. Res. 14 (2021) 4313–4328.

[12] A. Aita, D. Basso, A.M. Cattelan, P. Fioretto, F. Navaglia, F. Barbaro, A. Stoppa, E. Coccorullo, A. Farella, A. Socal, R. Vettor, M. Plebani, SARS-CoV-2 identification and IgA antibodies in saliva: one sample two tests approach for diagnosis, Clin. Chim. Acta 510 (2020) 717–722.

[13] K. Sogbesan, T. Sogbesan, D.J. Hata, E.L. White, W. Daniel, S.L. Gasson, et al., Use of self-collected saliva samples for the detection of SARS-CoV-2, Lab. Med. (2022), https://doi.org/10.1093/labmed/lmac051.

[14] S.A. Kiryanov, T.A. Levina, V.V. Kadochnikova, M.V. Konopleva, A.P. Suslov, D.Y. Trofimov, Clinical evaluation of nasopharyngeal, oropharyngeal, nasal swabs, and saliva for the detection of SARS-CoV-2 by direct RT-PCR, Diagnostics (Basel) 12 (2022) 1091, https://doi.org/10.3390/diagnostics12051091.

[15] A. Jenney, D. Chibo, M. Batty, J. Druce, R. Melvin, A. Stewardson, A. Dennison, S. Symes, P. Kinsella, T. Tran, C. Mackenzie, D. Johnson, I. Thevarajan, C. McGrath, A. Matlock, J. Prestedge, M. Gooey, J. Roney, J. Bobbitt, S. Yallop, M. Catton, D.A. Williamson, Surveillance testing using salivary RT-PCR for SARS-CoV-2 in managed quarantine facilities in Australia: a laboratory validation and implementation study, Lancet Reg. Health - Western Pac. 26 (2022), 100533.

[16] D. Esser, G. Alvarez-Llamas, M.P. de Vries, D. Weening, R.J. Vonk, H. Roelofsen, Sample stability and protein composition of saliva: implications for its use as a diagnostic fluid, Biomark Insights 3 (2008) 25–27.

[17] D. Basso, A. Aita, A. Padoan, C. Cosma, F. Navaglia, S. Moz, N. Contran, C.-F. Zambon, A. Maria Cattelan, M. Plebani, Salivary SARS-CoV-2 antigen rapid detection: a prospective cohort study, Clin. Chim. Acta 517 (2021) 54–59.

[18] V. Scalcon, A. Folda, M.G. Lupo, F. Tonolo, N. Pei, I. Battisti, N. Ferri, G. Arrigoni, A. Bindoli, A. Holmgren, L. Coppo, M.P. Rigobello, Mitochondrial depletion of glutaredoxin 2 induces metabolic dysfunction-associated fatty liver disease in mice, Redox Biol. 51 (2022), 102277.

[19] S. Tyanova, T. Temu, J. Cox, The MaxQuant computational platform for mass spectrometry-based shotgun proteomics, Nat. Protoc. 11 (12) (2016) 2301–2319.

[20] Uniprot Database, 2022. https://www.uniprot.org/help/uniprotkb (accessed 19 July 2022).

[21] K.J. Adams, B. Pratt, N. Bose, L.G. Dubois, L. St. John-Williams, K.M. Perrott, K. Ky, P. Kapahi, V. Sharma, M.J. MacCoss, M.A. Moseley, C.A. Colton, B.X. MacLean, B. Schilling, J.W. Thompson, Skyline for small molecules: a unifying software package for quantitative metabolomics, J. Proteome Res. 19 (4) (2020) 1447–1458.

[22] SRMAtlas database, 2022, https://www.srmatlas.org (accessed 19 July 2022).

[23] STRING, 2022, https://www.string-db.org (accessed 19 July 2022).

[24] g:Profiler, 2022, https://biit.cs.ut.ee/gprofiler/gost (accessed 19 July 2022).

[25] Revigo, 2022, https://revigo.irb.hr (accessed 19 July 2022).

[26] J. Xu, Y. Li, F. Gan, Y. Du, Y. Yao, Salivary glands: potential reservoirs for COVID-19 asymptomatic infection, J. Dent. Res. 99 (8) (2020) 989.

[27] R. Xu, B. Cui, X. Duan, P. Zhang, X. Zhou, Q. Yuan, Saliva: potential diagnostic value and transmission of 2019-nCoV, Int. J. Oral Sci. 12 (1) (2020) 11.

[28] F. Amado, M.J.C. Lobo, P. Domingues, J.A. Duarte, R. Vitorino, Salivary peptidomics, Expert Rev. Proteomics 7 (5) (2010) 709–721.

[29] B. Manconi, M. Castagnola, T. Cabras, A. Olianas, A. Vitali, C. Desiderio, M.T. Sanna, I. Messana, The intriguing heterogeneity of human salivary proline-rich proteins: Short title: Salivary proline-rich protein species, J. Proteomics 134 (2016) 47–56.

[30] E. Delva, D.K. Tucker, A.P. Kowalczyk, The desmosome, Cold Spring Harbor Perspect. Biol. 1 (2) (2009), a002543.

[31] C. Toelzer, K. Gupta, S.K.N. Yadav, U. Borucu, A.D. Davidson, M. Kavanagh Williamson, D.K. Shoemark, F. Garzoni, O. Staufer, R. Milligan, J. Capin, A.J. Mulholland, J. Spatz, D. Fitzgerald, I. Berger, C. Schaffitzel, Free fatty acid binding pocket in the locked structure of SARS-CoV-2 spike protein, Science 370 (6517) (2020) 725–730.

[32] V.J. Costela-Ruiz, R. Illescas-Montes, J.M. Puerta-Puerta, C. Ruiz, L. Melguizo-Rodríguez, SARS-CoV-2 infection: the role of cytokines in COVID-19 disease, Cytokine Growth Factor Rev. 54 (2020) 62–75.

[33] L. Chen, X. Long, Q. Xu, J. Tan, G. Wang, Y. Cao, J. Wei, H. Luo, H. Zhu, L. Huang, F. Meng, L. Huang, N. Wang, X. Zhou, L. Zhao, X. Chen, Z. Mao, C. Chen, Z. Li, Z. Sun, J. Zhao, D. Wang, G. Huang, W. Wang, J. Zhou, Elevated serum levels of S100A8/A9 and HMGB1 at hospital admission are correlated with inferior clinical outcomes in COVID-19 patients, Cell. Mol. Immunol. 17 (9) (2020) 992–994.

[34] A. Silvin, N. Chapuis, G. Dunsmore, A.-G. Goubet, A. Dubuisson, L. Derosa, C. Almire, C. Hénon, O. Kosmider, N. Droin, P. Rameau, C. Catelain, A. Alfaro, C. Dussiau, C. Friedrich, E. Sourdeau, N. Marin, T.-A. Szwebel, D. Cantin, L. Mouthon, D. Borderie, M. Deloger, D. Bredel, S. Mouraud, D. Drubay, M. Andrieu, A.-S. Lhonneur, V. Saada, A. Stoclin, C. Willekens, F. Pommeret, F. Griscelli, L.G. Ng, Z. Zhang, P. Bost, I. Amit, F. Barlesi, A. Marabelle, F. Pène, B. Gachot, F. André, L. Zitvogel, F. Ginhoux, M. Fontenay, E. Solary, Elevated calprotectin and abnormal myeloid cell subsets discriminate severe from mild COVID-19, Cell 182 (6) (2020) 1401–1418.e18.

[35] L. Mellett, S.A. Khader, S100A8/A9 in COVID-19 pathogenesis: impact on clinical outcomes, Cytokine Growth Factor Rev. 63 (2022) 90–97.

[36] S. Wang, R. Song, Z. Wang, Z. Jing, S. Wang, J. Ma, S100A8/A9 in inflammation, Front Immunol. 9 (2018) 1298.

[37] A. Muñoz-Prieto, I. Rubić, J.C. Gonzalez-Sanchez, J. Kuleš, S. Martínez-Subiela, J.J. Cerón, et al., Saliva changes in composition associated to COVID-19: a preliminary study, Sci. Rep. 12 (2022) 10879.

[38] M. Mrag, H. Hamdouni, A. Gouiaa, A. Omezzine, F. Ben Amor, A. Kassab, Investigation of carbonic anhydrase 6 gene polymorphism rs2274327 in relation to the oral health status and salivary composition in type 2 diabetic patients, Acta Odontol. Scand. 78 (8) (2020) 560–564.

[39] L. Rodrigues, R. Espanca, A.R. Costa, C.M. Antunes, C. Pomar, F. Capela-Silva, C.C. Pinheiro, P. Domingues, F. Amado, E. Lamy, Comparison of salivary proteome of children with different sensitivities for bitter and sweet tastes: association with body mass index, Int. J. Obes. 43 (4) (2019) 701–712.

[40] M. Kloc, A. Uosef, J. Wosik, J.Z. Kubiak, R.M. Ghobrial, Virus interactions with the actin cytoskeleton—what we know and do not know about SARS-CoV-2, Arch. Virol. 167 (3) (2022) 737–749.

[41] S. Elahi, Hematopoietic responses to SARS-CoV-2 infection, Cell. Mol. Life Sci. 79 (3) (2022) 187.